Mecánica Computacional Vol. XXII
M. B. Rosales, V. H. Cortínez y D. V. Bambill (Editores)
Bahía Blanca, Argentina, Noviembre 2003.

MIXED CONVECTION IN AN INCLINED CHANNEL WITH A DISCRETE HEAT SOURCE

Paulo M. Guimarães* and Genésio J. Menon†

***** Departamento de Engenharia Mecânica,Universidade Federal de Itajubá – UNIFEI
Av. BPS, 1303, Pinheirinho, 37500-176 - Itajubá - MG – Brasil. TE: 00 55 35 3629-1163
e-mail: paulomgui@uol.com.br, web page: http://www.unifei.edu.br

† Departamento de Engenharia Mecânica,Universidade Federal de Itajubá – UNIFEI
Av. BPS, 1303, Pinheirinho, 37500-176 - Itajubá - MG – Brasil. TE: 00 55 35 3629-1163
e-mail: genesio@iem.efei.br, web page: http://www.unifei.edu.br

Key words: Finite Element Method, Heat Source, Petrov-Galerkin, Mixed Convection

Abstract. *In this work, it is studied the mixed convection in an inclined rectangular channel. A constant-flux heat source q of finite length is placed on the lower surface of the channel, while its remaining part is adiabatic. The upper surface in contact with the fluid is kept at a constant cold temperature T_c . At the inlet, it is imposed a constant velocity profile U_o as well as a constant temperature T_o profile. The ranges performed have been as follows: $1 \leq Re \leq 500$, $10^3 \leq Gr \leq 10^5$, and $0° \leq \gamma \leq 90°$. The set of governing equations have been discretized and solved using the Galerkin finite element method with the Penalty formulation in the pressure terms and the Petrov-Galerkin perturbations in the convective terms. Two comparisons have been performed to validate the computational code. It has been shown that the effect of the inclination angle on the velocity and temperature distributions plays an important role on the heat transfer for low Re and high Gr. For high Re, the effect of the orientation is negligible. In general, it has also been discovered that an inclination angle around 60° and 75° provide the most desirable work conditions when cooling is aimed. Some cases have presented the reversed flow for low Re and high Gr. The flow reversal does not noticeably influence the heat transfer coefficient on the module. The results shown here encourage the use of inclined boards in cabinets, however some other geometrical aspects should be accounted.*

1 INTRODUCTION

Knowledge in natural, mixed, and forced convection in inclined channels, has been accumulated in previous works in literature because of its practical applications including electronic systems, high performance heat exchangers, chemical process equipments, combustion chambers, environmental control systems, and so forth. These kinds of flows are complex because they involve separations, re-attachments, and recirculations of the flow influenced by changes in the geometry and by the presence of thermal conditions. For instance, in a channel with a pressure-driven external flow, the increasingly high heat flux from electronic modules heightens the possibility of complex flows due to the buoyancy effects. It is important therefore to understand the interaction between buoyancy-induced flow and pressure-driven external flow, and the corresponding heat transfer features in a channel.

Bae and Hyun[1] carry out a study for the time-dependent laminar natural convection air cooling in a vertical rectangular enclosure with three discrete flush-mounted heaters. The results show the influence of the time-dependent thermal condition of the lowest-elevation heater on the temperature of the other heaters. The evolutions of global flow and temperature fields are exemplified to provide physical interpretations. The study emphasizes that the transient-stage temperatures at the heaters can exceed the corresponding steady-state values. This is relevant to practical design of electronic devices.

Madhavan and Sastri[2] demonstrate a parametric study for a conjugate natural convection cooled substrate mounted heat sources placed inside an enclosure. This particular situation has direct relevance in electronic cooling applications. It is found that Ra, Pr, and enclosure boundary condition affect strongly the fluid flow and heat transfer characteristics. It is concluded that non-dimensional temperature is maximum for Pr = 150. Numerical correlation for maximum protrusion temperature and Nusselt number are presented for a wide range of Pr, Ra, and enclosure boundary conditions.

Choi and Ortega[3] investigate numerically using the finite difference method the effects of laminar forced flow on buoyancy-induced natural convection cells throughout the regions of natural, mixed, and forced convection for parallel planes channel with a discrete heat source. Emphasis is placed on the influence of the inlet flow velocity and the inclination angle of the channel, and the local buoyancy induced by the discrete source. The results indicate that the overall Nusselt number of the source strongly depends on the inclination angle (γ- according to their convention- 0° corresponds to the vertical aiding position) in the natural and mixed convection regimes when $\gamma > 45°$. On the other hand, the changes in Nu and θ_{max} are negligible when the channel is from 0° to 45°, i.e., there is no significant penalty in heat transfer due to the inclination of the channel up to $\gamma = 45°$. As Gr increases at a fixed Re, an entrainment of the air from the downstream exit is observed for the case of aiding flow. This paper is taken as the basis for the present work which studies the thermal and flow pattern in more detail for more inclination angles between 0° and 90° (according to the present work 0° represents the horizontal position and 90°, the vertical aiding one). Peterson and Ortega[4] present a complete review of the channel flow problem applied to electronics.

Conjugate mixed convection from a discrete thermal source or multiple sources in a rectangular cavity is investigated by Papanicolau and Jaluria[5,6]. They observed that the

location of the source on the right vertical wall is the most favorable in terms of cooling, and that oscillatory flow and thermal fields may develop in the enclosure depending on the relative location of the components at high inputs by the components.

Kennedy and Zebib[7] present results on the effects of free and forced laminar horizontal channel flow with a discrete heat source located on either the upper or the lower wall, and two heat sources on both walls. They suggest several guidelines for their thermal design of the electronic packages based on a comparison of the results.

The present work carries out the influence of the buoyancy-assisting flow in a single inclined channel with a discrete source. Vertical and horizontal channels are also considered. Special emphasis is given to the maximum surface temperature on the module in addition to the overall heat transfer features due to the importance of the thermal control in electronic packages to keep the component temperature below the manufacturer's maximum specified operating temperature.

2 PROBLEM DESCRIPTION

In this work, it is studied the mixed convection in an inclined rectangular channel with height H and length L. A constant-flux heat source q of finite length B is placed between x_1 and x_2 on the lower surface of the channel, while its remaining part is adiabatic. The upper surface in contact with the fluid is kept at a constant cold temperature T_c . At the inlet, it is imposed a constant velocity profile U_o as well as a constant temperature T_o profile. As for the open boundary condition OBC, it is considered to be convective and time dependent. In fact, in the method applied here, the open boundary conditions are arranged in a way that they are calculated. Therefore, nothing is directly applied at the open boundary. Throughout this work the geometry studied has x_1 = 5H, x_2 = 6H, B=H, and L = 15H. The temperatures T_o and T_c are assumed to be the same.

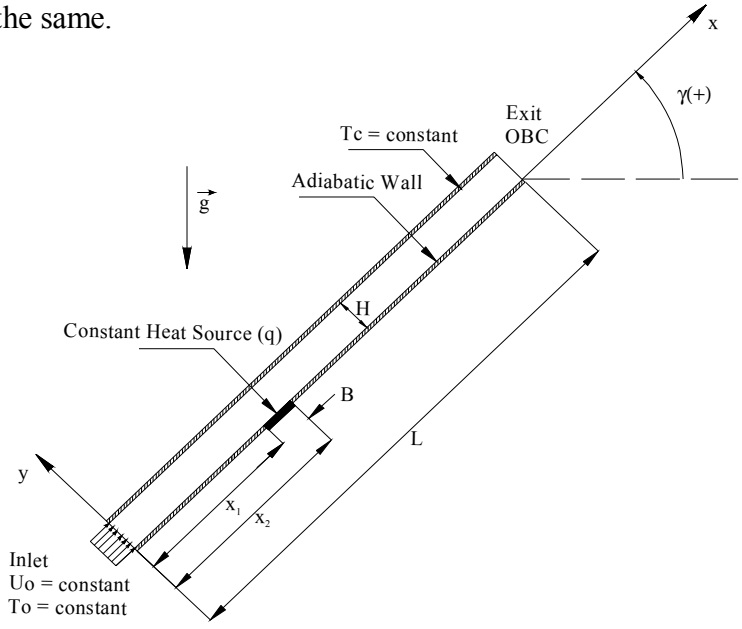

Figure 1. Channel geometry and boundary conditions.

3 PROBLEM FORMULATION

The problem governing equations are given by the equations of mass conservation, Navier-Stokes, and energy. Being that u and v are the velocity components, T is the fluid temperature, t' is the time field, D_T is the thermal diffusivity, β_T is the thermal expansion coefficient, ν is the kinematic viscosity, g is the gravitational acceleration, ρ_0 is the fluid density and T_0 is the reference temperature taken as $T_0 = T_c$.

Under the Boussinesq approximation and the following dimensionless parameters:

$$X=\frac{x}{B};\quad Y=\frac{y}{B};\quad U=\frac{u}{U_o};\quad V=\frac{v}{U_o};\quad P=\frac{p}{\rho_0 {U_o}^2};\quad t=\frac{t'}{(B/U_o)};\quad \theta=(T-T_o)/(q'B/D_T);$$

$$Fr=\frac{Re^2}{Gr}=\frac{{U_o}^2}{\beta_T g\Delta T B};\quad Pr=\frac{\nu}{D_T};\quad Gr=\frac{\beta_T g\Delta T B^3}{\nu^2};\quad Re=\frac{U_o\rho_0 B}{\mu};\quad \Delta T=T_h-T_c \tag{1}$$

where Fr, Pr, Gr, Re, Um, and μ are, respectively, the Froude number, the Prandtl number, the Grashof number, the Reynolds number, the average velocity, and the dynamic viscosity, the dimensionless governing equations can be cast into the following form:

$$\frac{\partial U}{\partial X}+\frac{\partial V}{\partial Y}=0; \tag{2}$$

$$\frac{\partial U}{\partial t}+U\frac{\partial U}{\partial X}+V\frac{\partial U}{\partial Y}=-\frac{\partial P}{\partial X}+\frac{1}{Re}\left(\frac{\partial^2 U}{\partial X^2}+\frac{\partial^2 U}{\partial Y^2}\right)+\sin(\gamma)\frac{\theta}{Fr}; \tag{3}$$

$$\frac{\partial V}{\partial t}+U\frac{\partial V}{\partial X}+V\frac{\partial V}{\partial Y}=-\frac{\partial P}{\partial Y}+\frac{1}{Re}\left(\frac{\partial^2 V}{\partial X^2}+\frac{\partial^2 V}{\partial Y^2}\right)+\cos(\gamma)\frac{\theta}{Fr}; \tag{4}$$

$$\frac{\partial \theta}{\partial t}+U\frac{\partial \theta}{\partial X}+V\frac{\partial \theta}{\partial Y}=\frac{1}{Re\,Pr}\left(\frac{\partial^2 \theta}{\partial X^2}+\frac{\partial^2 \theta}{\partial Y^2}\right). \tag{5}$$

The boundary conditions are as follows:

$$U=V=0 \quad \text{(all walls)};\ \theta=0 \ \text{(entrance and upper wall)};\ U=1 \ \text{(entrance)}$$

$$q=-\frac{1}{Pe}\frac{\partial \theta}{\partial Y} \ \text{ with } \ \frac{\partial \theta}{\partial Y}=-1 \ \text{(on the source module).}$$

By applying the Petrov-Galerkin formulation to the equations above, Eqs. (2) to (5), together with the Penalty technique , the weak form of the conservation equations i as follows:

$$\int_\Omega N_i\left[\frac{\partial U}{\partial t}+\frac{1}{Re}\left(\frac{\partial N_i}{\partial X}\frac{\partial U}{\partial X}+\frac{\partial N_i}{\partial Y}\frac{\partial U}{\partial Y}\right)\right]d\Omega+\int_\Omega^R \lambda\frac{\partial N_i}{\partial X}\left(\frac{\partial U}{\partial X}+\frac{\partial V}{\partial Y}\right)d\Omega=$$

$$\int_\Omega\left[(N_i+P_{i1})\left(U\frac{\partial U}{\partial X}+V\frac{\partial U}{\partial Y}\right)+N_i\sin(\gamma)\frac{\theta}{Fr}\right]d\Omega-\int_{\Gamma_0} N_i\,p\,n_x\,d\Gamma \tag{6}$$

$$\int_\Omega N_i\left[\frac{\partial V}{\partial t}+\frac{1}{Re}\left(\frac{\partial N_i}{\partial X}\frac{\partial V}{\partial X}+\frac{\partial N_i}{\partial Y}\frac{\partial V}{\partial Y}\right)\right]d\Omega+\int_\Omega^R \lambda\frac{\partial N_i}{\partial Y}\left(\frac{\partial U}{\partial X}+\frac{\partial V}{\partial Y}\right)d\Omega=$$

$$\int_\Omega\left[\left(N_i+P_{i1}\right)\left(U\frac{\partial V}{\partial X}+V\frac{\partial V}{\partial Y}\right)+N_i\cos(\gamma)\frac{\theta}{Fr}\right]d\Omega-\int_{\Gamma_0}N_i\,p\,n_y\,d\Gamma \tag{7}$$

$$\int_\Omega\left[N_i\frac{\partial\theta}{\partial t}+\frac{1}{Re\,Pr}\left(\frac{\partial N_i}{\partial X}\frac{\partial\theta}{\partial X}+\frac{\partial N_i}{\partial Y}\frac{\partial\theta}{\partial Y}\right)\right]d\Omega=\int_\Omega\left(N_i+P_{i2}\right)\left(U\frac{\partial\theta}{\partial X}+V\frac{\partial\theta}{\partial Y}\right)d\Omega+\int_{\Gamma_1}N_i\,q\,d\Gamma \tag{8}$$

where the dependent variables are approximated by:

$$\Phi(X,Y,t)=\sum_j N_j(X,Y)\Phi_j(t)\ ;\ p(X,Y,t)=\sum_k M_k(X,Y)p_k(t)\ . \tag{9}$$

N_i and N_j denote the linear shape functions for Φ, that is, for U, V, and θ, and M_k denotes the shape functions for the constant piecewise pressure. P_{ij} are the Petrov-Galerkin perturbations applied to the convective terms only. The terms P_{ij} are defined as follows:

$$P_{ij}=k_j\left(U\frac{\partial N_i}{\partial X}+V\frac{\partial N_i}{\partial Y}\right);\ k_j=\frac{\alpha_j\bar{h}}{|V|}\ ;\ \alpha_j=\coth\frac{\gamma_j}{2}-\frac{2}{\gamma_j};\quad \gamma_j=\frac{|V|\bar{h}}{\varepsilon_j};\ j=1,2 \tag{10}$$

where γ is the element Péclet number, $|V|$ is the absolute value of the velocity vector that represents the fluid average velocity within the each element, $\bar{h}$ is the element average size, $\varepsilon_1=1/Re, \varepsilon_2=1/Pe$, and λ is the Penalty parameter which is considered to be 10^9. The time integration is by a semi-implicit backward Euler method. Moreover, the convective terms are calculated explicitly and the viscous and Penalty terms implicitly. The temperatures and velocities are interpolated by using the four-noded quadrilateral elements and the pressure by the one-noded ones. Finally, the reduced integration is applied to the penalty term to avoid numerical locking.

The average Nusselt number along a surface S can be written as:

$$Nu=\frac{1}{S}\int_S\left[\frac{1}{\theta}\right]ds\ . \tag{11}$$

The algorithm is validated by comparing the results of the present work with both the ones obtained in experimental and numerical investigations. Figures (2) and (3) show the geometries and the boundary conditions used in the first and second comparisons, respectively.

The first comparison is accomplished not only by using the experimental results presented by Lee and Mateescu[8] and Armaly[9] et al., but also by the numerical ones achieved by Lee and Mateescu[8], Gartling[10], Kim and Moin[11], and Sohn[12]. The air flow of the present comparison analysis is taken as bidimensional, laminar, incompressible, and under the unsteady regime. The domain is a horizontal upstream backward-facing step channel whose inlet has a fully developed velocity profile given by u = 24y(0.5-y) $\bar{U}$ and v = 0 in which Re

= 800. The computational domain is shown in Fig. (2) where all walls are under the no-slip condition.

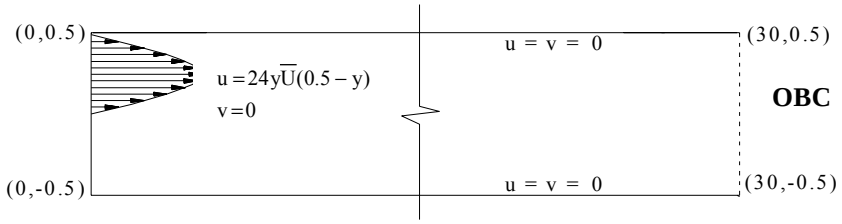

Figure 2. Geometry and boundary conditions for the first comparison.

Table (1) shows the results from the first comparison for the flow separation distance Xs on the upper surface and its reattachment distance Xrs. As for the bottom surface, the comparison is made on the reattachment distance Xr. As it can be noticed, the results of the present work agree well with the ones from the literature.

Table1. Comparison of computed predictions and experimental measurements of dimensionless lengths (with respect to the channel height) of separation and reattachment on upper and lower walls.

		Experimental results			Computed results			
	Length on	Lee and Mateescu[8]	Armaly[9] et al.	Present prediction	Gartling[10]'s prediction	Kim & Moin[11]	Lee and Mateescu[8]	Sohn[12]
Lower Wall	x_r	6.45	7.0	5.75	6.1	6.0	6.0	5.8
Upper Wall	x_s	5.15	5.7	4.95	4.85	-	4.8	-
	x_{rs}	10.25	10.0	9.9	10.48	-	10.3	-
	x_{rs}-x_s	5.1	4.3	4.95	5.63	5.75	5.5	4.63
Reynolds		805	800	800	800	800	800	800
Hd/Hu		2	1.94	2	2	2	2	2

The second comparison is performed with the numerical results shown by Comini[13] et all. The contrasting study is carried out by considering a problem involving mixed convective heat transfer with the flow being bidimensional, laminar, and incompressible in the unsteady

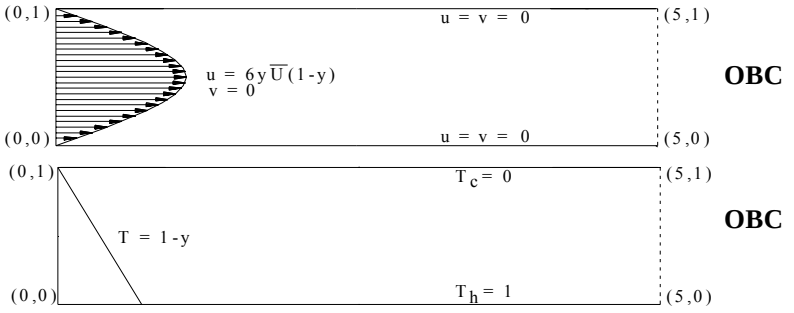

Figure 3. Geometry and boundary conditions for the second comparison.

regime. In this case, some values are chosen such as Re=10, Pr = 0.67, and Fr = 1/150. The grid has 4000 quadrilateral four-noded elements with $\Delta x = 0.1$, $\Delta y = 0.15$, $\Delta t = 0.01$ and 1000 iterations. Figure (4) displays the average Nusselt number on the upper surface versus time. After approximately iteration 500, the regime turns to be periodic with the average Nusselt number on the upper wall oscillating around a mean value of 2.44. This value agrees satisfactorily with the one found by Comini[13] et all which is 2.34, resulting in a deviation of about 4%.

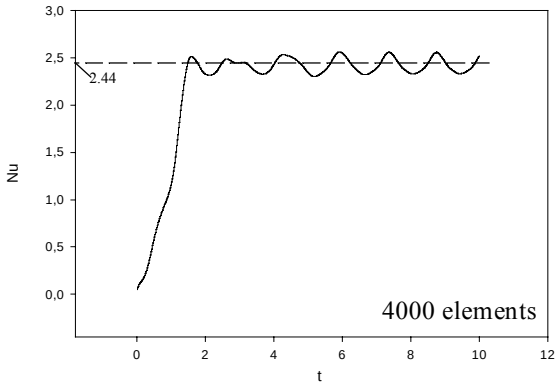

Figure 4. Average Nusselt number Nu measured along the upper surface versus time for a Poiseuille flow heated from below.

4 RESULTS

Figure (5) shows the isotherm distributions considering the ranges for the Reynolds number (Re), the Grashof number (Gr), and the inclination angle, respectively, as $1 \leq Re \leq 10$, $10^3 \leq Gr \leq 10^5$, and $0° \leq \gamma \leq 90°$. By observing the isotherms from Fig. (5), the orientation of the channel has a significant effect on the temperature distribution for lower Re, that is, Re = 1, 5, and 10. This effect is even stronger when Gr increases. Later on this paper, this effect on the Nusselt number will be seen. On the other hand, for higher Reynolds over 50 or so (not shown in Fig. (5)), the inclination angle has a weaker effect on the temperature distributions.

Figure (6) shows the effect of the source module on the velocity distributions for the horizontal cases ($\gamma = 0°$) with Re = 1, 5, and 10, considering $Gr = 10^5$. It can be noted that in the natural convection regime, the thermal plume is approximately symmetric about the centerline of the module (Fig. 5). In the plume region there are two opposite recirculating cells almost symmetric. Moreover, as Re increases the plume shifts and stretches towards the downstream. This effect features how the natural convection starts to vanish, giving place to the mixed convection. If Re increases more, for instance, $Re \geq 100$ (not shown in Fig. (6)), the forced convection dominates the flow pattern and the heat transfer process.

One can note in the temperature distribution along the module in Fig. (7), for $Gr = 10^5$, and Re= 1, 5, 10, the transition from the natural convection to the mixed convection. As Re is higher, the maximum temperature on the module decreases. This is due to the fact that when higher velocities are present, the cell recirculation gets further from the module allowing a bigger contact of the cold fluid with the module.

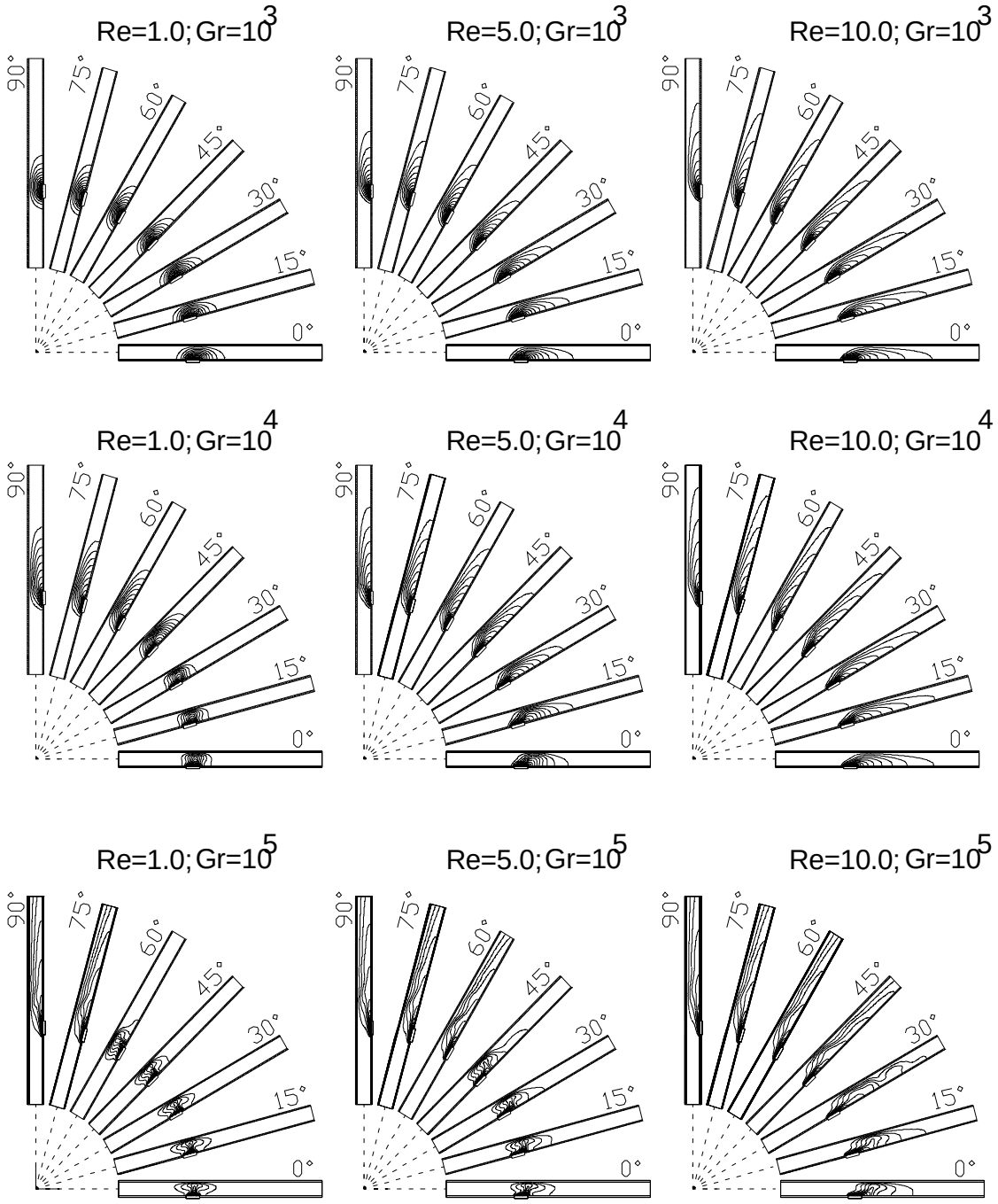

Figure 5. Isotherms for Gr = 10^3, 10^4, 10^5; Re = 1, 5 , 10; and γ = 0°, 15°, 30°, 45°, 60°, 75°, 90°.

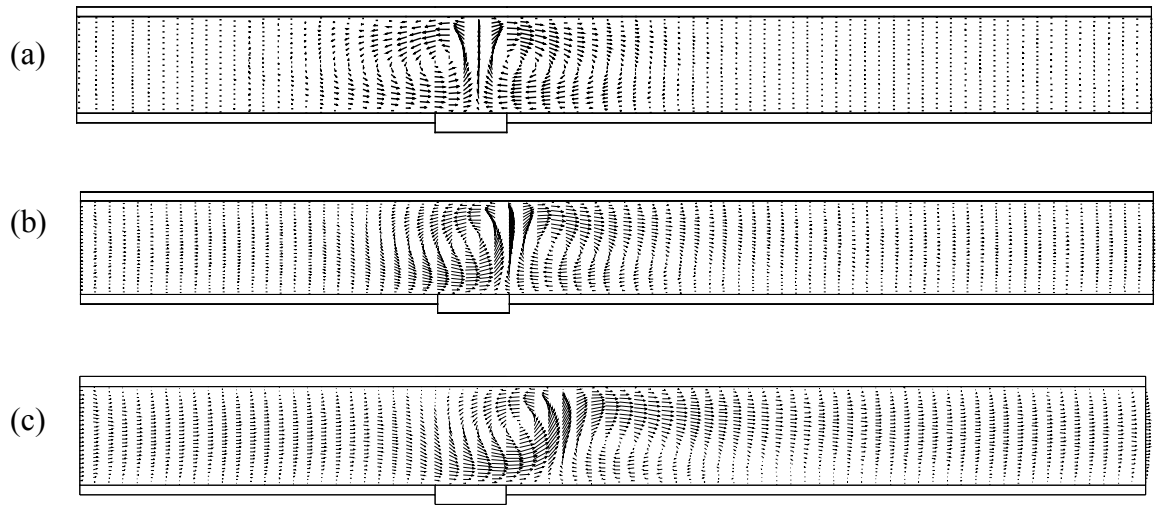

Figure 6. Velocity distributions for Gr = 10^5, $\gamma = 0°$, and Re = (a) 1, (b) 5, and (c) 10.

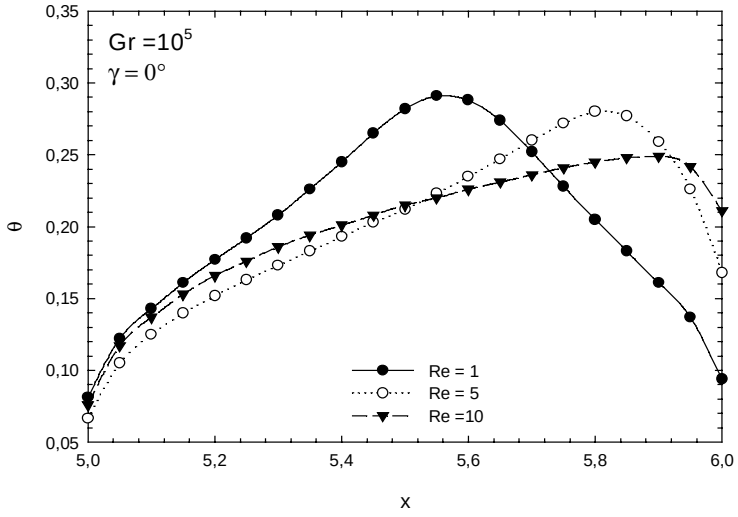

Figure 7. Module temperature distributions for Gr = 10^5, $\gamma = 0°$ and Re = 1, 5, and 10.

Figure (8) depicts the velocities for Gr = 10^5 and Re = 1, 5, and 10, for $\gamma = 45°$. As Re increases, the clockwise recirculating cell tends to vanish, whereas the anticlockwise ones tend to dominate to an extent that reversed flow exists at the exit. The presence of the flow reversal does not necessarily imply an increase of the Nusselt number on the module. It is interesting to observe the formation of secondary recirculating cells in Fig. (8c), and that as a result of this formation, the corresponding isothermal lines are distorted, as shown in Fig. (5). In Fig. (8b) the reversal flow is almost happening. Comparing Fig. (8) with Fig. (6), there is a subtle difference in the velocity vectors, hence showing the effect of the orientation of the channel.

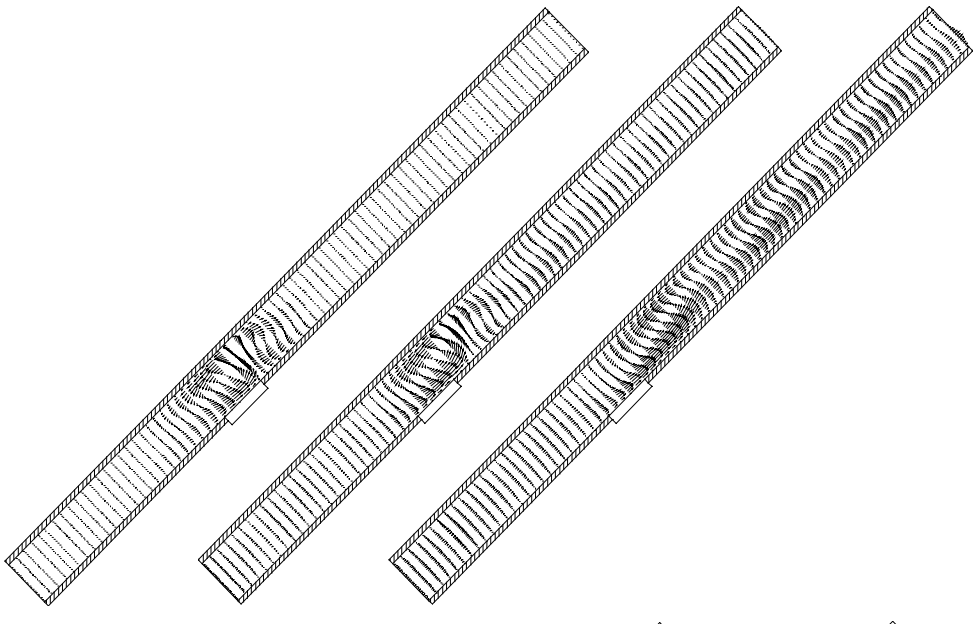

(a) (b) (c)

Figure 8. Velocity distributions for Gr = 10^5, $\gamma = 45°$, and Re = (a) 1, (b) 5, and (c) 10.

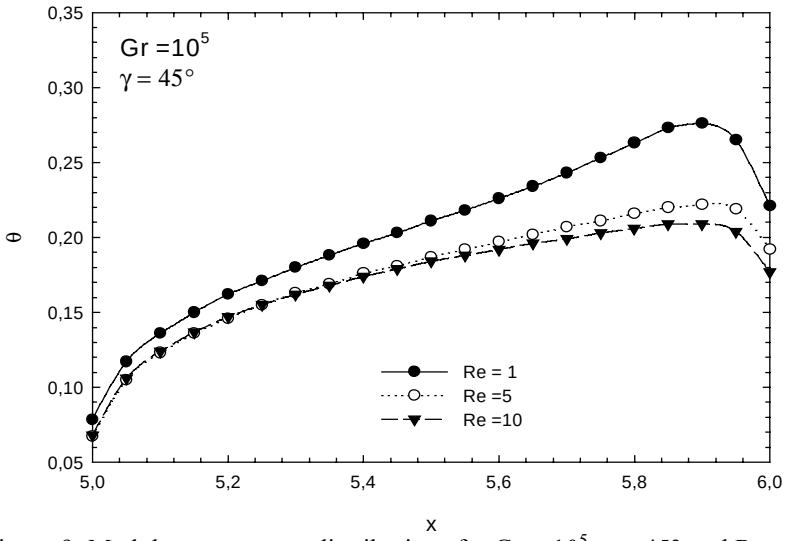

Figure 9. Module temperature distributions for Gr = 10^5, $\gamma = 45°$ and Re = 1, 5, and 10.

In Figure (9), the temperature distributions along the module are shown for the cases from Fig.(8a-c). In a general way, the maximum temperature on the module decreases for the three cases. It must be remembered that the ideal work conditions in equipments with electronic circuit boards are those in which the module presents the lowest values for the maximum temperature. Therefore, having these conditions in mind, the increase of the inclination angle provides lower values for the maximum temperature.

Figure (10) presents the velocity distributions for Gr = 10^5, Re = 1, 5, and 10, but now with the channel on the vertical position, $\gamma = 90°$. It can be noted that for all the values of Re, there is a flow reversal at the outlet that is stronger than the reversed flow for $\gamma = 45°$. For each of these three cases in Fig. (10) , there is a secondary recirculating cell.

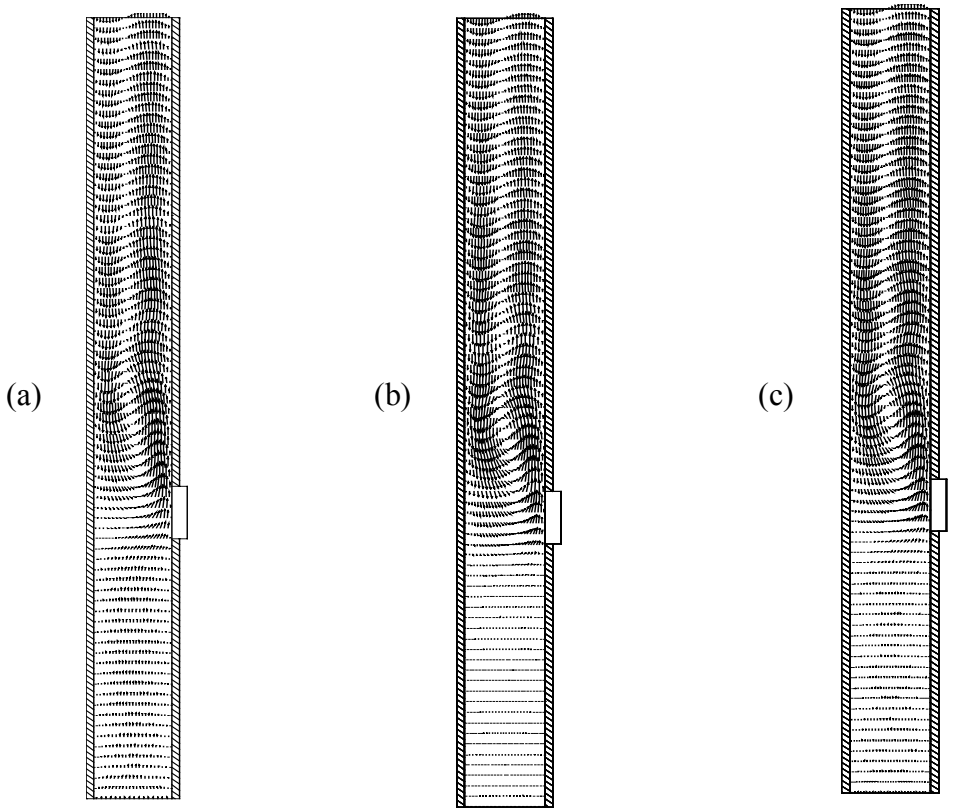

Figure 10. Velocity distributions for Gr = 10^5, $\gamma = 90°$, and Re = (a) 1, (b) 5, and (c) 10.

Figure (11) shows that there is not a significant difference in the temperature on the module for the Reynolds values Re = 1, 5, and 10; Gr = 10^5, and $\gamma = 90°$.

Figure (12) makes a comparison of the Nusselt numbers for $1 \leq Re \leq 500$, $0° \leq \gamma \leq 90°$ and for the three Grashof numbers Gr =10^3, 10^4, and 10^5. These results are in good agreement with those found by Choi and Ortega[3]. In the work of Choi and Ortega[3] it was observed according to the 'five percent deviation rule' suggested by Sparrow[14] et al., that the natural, mixed, and forced convection can be determined. From Figs. (12a-c), the same is found here, where the mixed convection regimes are, approximately, within the ranges $1 < Re < 50$ for Gr = 10^3, $5 < Re < 100$ for Gr = 10^4, and $10 < Re < 500$ for Gr = 10^5. Practically, there is no reduction in the Nusselt number in these cases where the aiding flow is present, which also agrees with Choi and Ortega[3]. It can be noted that the collapse of the curves at high Re

explains that the buoyancy effects and, therefore, the influence of inclination diminish as forced convection dominates.

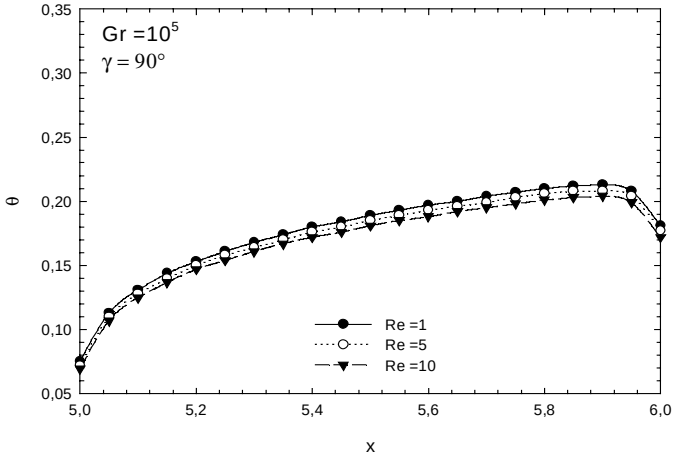

Figure 11. Module temperature distributions for Gr = 10^5, γ = 90° and Re = 1, 5, and 10.

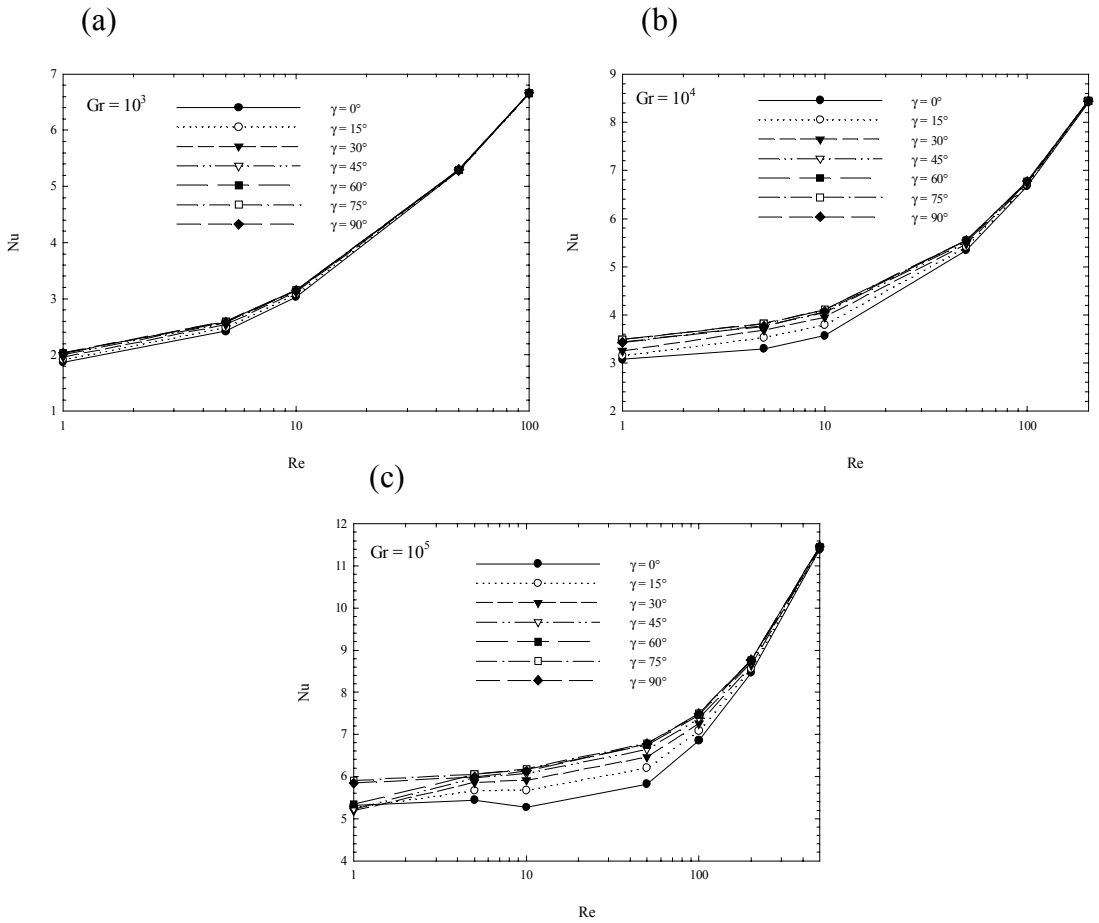

Figure 12. Average Nusselt number versus Re for 0° ≤ γ ≤ 90°, Gr = (a) 10^3, (b) 10^4, and (c) 10^5.

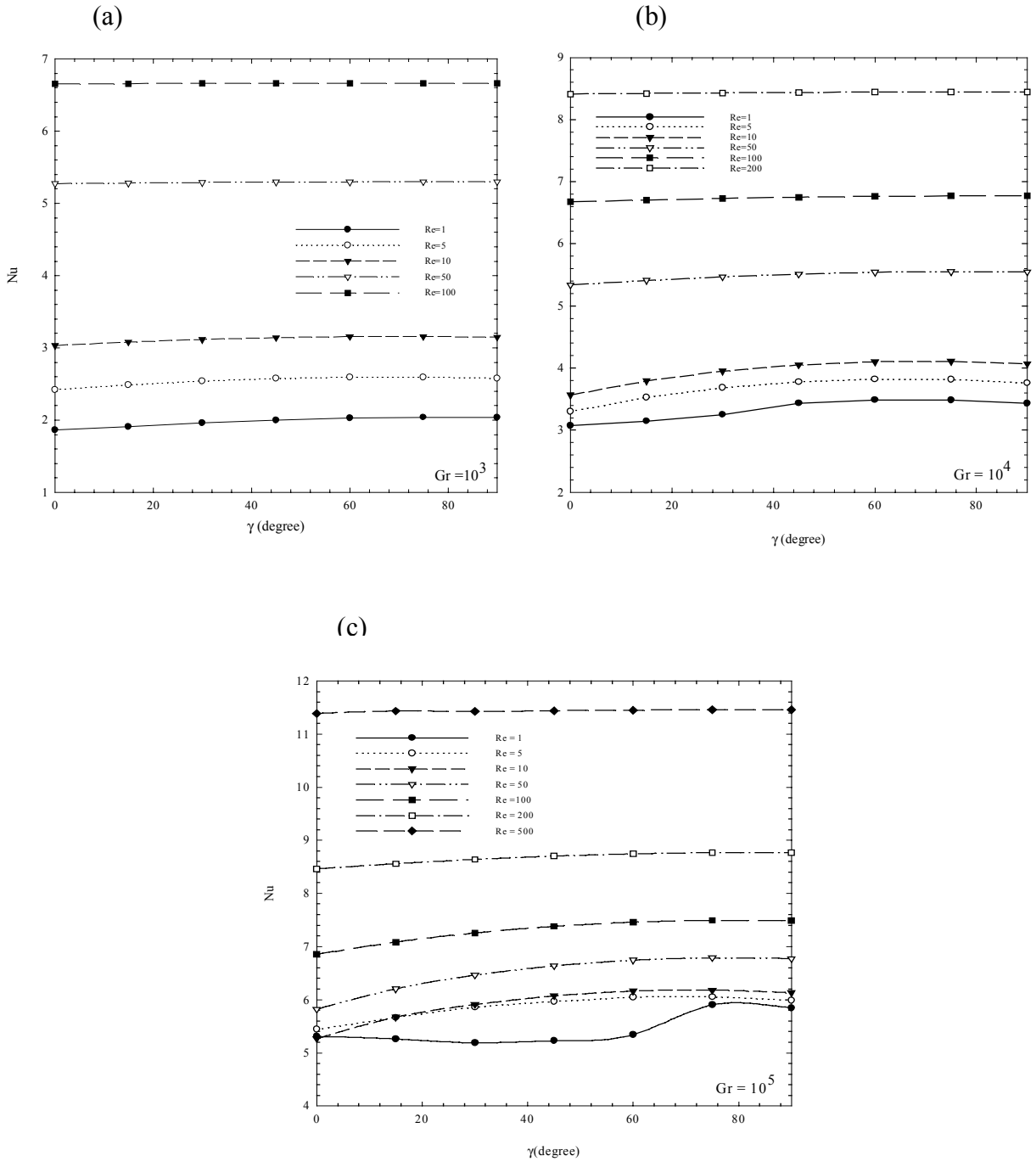

Figure 13. Average Nusselt versus γ for $1 \leq Re \leq 500$ and Gr = (a) 10^3, (b) 10^4, and (c) 10^5.

Figure (13) shows the influence of the orientation angle in the heat transfer for all the cases studied in this work, that is, Re = 1, 5, 10, 50, 100, 200, 500; γ = 0°, 15°, 30°, 45°, 60°, 75°, 90°; and Gr = 10^3, 10^4, and 10^5. In a general way, Nu is strongly dependent on the orientation of the channel in the limits of the natural and forced convection. For instance, when Gr = 10^3, the natural convective cells are not sufficiently strong to influence the flow and the temperature fields (Fig. 5), that means that the heat transfer mode involved is almost conductive. As Gr increases, the variations in Nu are more significant for low Re. In the work of Choi and Ortega[3], it is said that in the natural and mixed convection, the most suitable situation in the cooling of an electronic module, that is, the lowest Nu, is found when the channel orientation is in the range 45°<γ<90° (considering the convention adopted in the present work), in a general way. Analyzing Fig. (13), there is still a more favorable inclination within the range proposed by Choi and Ortega[3], which is around 60° and 75°. A situation that should be avoided would be when γ = 0°, in the natural and mixed convection. A particular case which provided a drastic increase in Nu, of course proportionally to the strengths involved here, is for Gr = 10^3 and Re = 1 in the range 60° ≤ γ ≤ 75°. This can also be noted in Fig. (5), in the isotherms distributions. Here, only γ = 75° presents a more appealing situation when cooling is the aim of a project, with a little difference when γ = 90°.

5 CONCLUSIONS

The mixed convection has been studied in a simple channel considering the effect of the inclination angle and some physical parameters. The ranges performed have been as follows: 1 ≤ Re ≤500, 10^3 ≤ Gr ≤10^5, and 0° ≤ γ ≤90°. The set of governing equations have been discretized and solved using the Galerkin finite element method with the Penalty formulation in the pressure terms and the Petrov-Galerkin perturbations in the convective terms. 5980 four-noded elements have been used to discretize the spatial domain. Two comparisons have been performed to validate the computational code. The first one has considered a horizontal upstream backward-facing step channel with isothermal flow and the second one has been a horizontal channel with Poiseuille flow heated from below. The two comparisons have agreed very well. It has been observed from the results of the present work that the effect of the inclination angle on the velocity and temperature distributions plays an important role on the heat transfer for low Re and high Gr. For high Re, the effect of the orientation is negligible. One must understand that when the words ‘low’ and ‘high’ are mentioned here, it means low and high compared to the limits considered in this work. In general, it has also been discovered that an inclination angle around 60° and 75° provides the most desirable work conditions when cooling is aimed. In Choi and Ortega[3] it was said that this optimal orientation would be 90°, despite no significant changes were found after γ = 45° (according to the convection adopted here). Some cases have presented the reversed flow for low Re and high Gr. The flow reversal does not noticeably influence the heat transfer coefficient on the module, although it does change the velocity and temperature fields significantly. In general, the results shown here encourage the use of inclined boards in cabinets, however it deserves more attention because some other aspects should be addressed such as the geometrical arrangement of the boards.

6 ACKNOWLEDGEMENTS

The authors acknowledge CAPES for its financial support without which this work would not be possible.

7 REFERENCES

[1] J.H. Bae and J.M. Hyun, "Time-dependent buoyant convection in an enclosure with discrete heat sources*", Int. J. Thermal Sciences*, **In press** (2003).
[2] P.N. Madhavan and V.M.K. Sastri, "Conjugate natural convection cooling of protruding heat sources mounted on a substrate placed inside an enclosure: a parametric study", *Comput. Methods Appl. Mech Engrg*., **188**, 187-202 (2000).
[3] C.Y. Choi and A. Ortega, "Mixed convection in an inclined channel with a discrete heat source", *Int. J. Heat Mass Transfer*, **36**, 3119-3134 (1993).
[4] G.P. Peterson and A. Ortega, "Thermal control of electronic equipment and devices", *Adv. Heat Transfer*, **20**, 181-314 (1990).
[5] E. Papanicolau and Y. Jaluria, "Conjugated mixed convection from thermal sources in a rectangular cavity", *Proc. ASME Winter Annual Meeting*, **HTD-57**, 29-40 (1990).
[6] E. Papanicolau and Y. Jaluria, "Forced and mixed convective cooling of multiple electronic components in an enclosure", *Proc. ASME/A.I.Ch.E. natl Conf.,* **HTD-171**, 20-37 (1991).
[7] K.J. Kennedy and A. Zebib, "Combined free and forced convection between horizontal parallel planes: some case studies", *Int. J. Heat Mass Transfer*, **26**, 471-474 (1983).
[8] T. Lee and D. Mateescu, "Experimental and numerical investigation of 2-D backward-facing step flow", *J. Fluids and Structures*, **12**, 703-716 (1998).
[9] B.F. Armaly, F. Durst, and J.C.F. Pereira & B. Schonung, "Experimental and theoretical investigation of backward-facing step flow", *J. Fluid Mechanics*, **127**, 473-496 (1983).
[10] D.K. Gartling, "A test problem for outflow boundary conditions – flow over a bachward-facinf step", *Int. J. Num. Meth. in Fluids*, **11**, 953-967 (1990).
[11] J. Kim and P. Moin, "Application of a fractional-step method to incompressible Navier-Stokes equations", *J. Comp. Physics*, **59**, 308-323 (1985).
[12] J. Sohn, "Evaluation of FIDAP on some classical laminar and turbulent benchmarks", *Int. J. Num. Meth. in Fluids*, **8**, 1469-1490 (1988).
[13] G. Comini, M. Manzam ,and G. Cortella, "Open boundary conditions for the streamfunction – vorticity formulation of unsteady laminar convection", *Num. Heat Transfer*, Part B, **31**, 217-234 (1997).
[14] E.M. Sparrow, R. Eichhorn, and J.L. Gregg, "Combined forced and free convection in a boundary layer", Phys. Fluids, **2**, 319-329 (1959).